Advanced Composite Materials
Publication details, including instructions for authors and subscription information:
http://www.tandfonline.com/loi/tacm20

Simplified Predictive Method of Viscosity of Nanofiber-Dispersed Polymer Suspensions

Tomohiro Yokozeki [a]

[a] Department of Aeronautics and Astronautics, The University of Tokyo, 7-3-1 Hongo, Bunkyo-ku, Tokyo 113-8656, Japan;, Email: yokozeki@aastr.t.u-tokyo.ac.jp

Version of record first published: 02 Apr 2012.

To cite this article: Tomohiro Yokozeki (2011): Simplified Predictive Method of Viscosity of Nanofiber-Dispersed Polymer Suspensions, Advanced Composite Materials, 20:6, 537-546

To link to this article: http://dx.doi.org/10.1163/156855111X610217

VSP

Advanced Composite Materials 20 (2011) 537–546

ADVANCED COMPOSITE MATERIALS
brill.nl/acm

Simplified Predictive Method of Viscosity of Nanofiber-Dispersed Polymer Suspensions

Tomohiro Yokozeki *

Department of Aeronautics and Astronautics, The University of Tokyo, 7-3-1 Hongo, Bunkyo-ku, Tokyo 113-8656, Japan

Received 26 July 2011; accepted 15 August 2011

Abstract

The viscosity of CNT-dispersed polymer suspensions is predicted based on elastic analogy. The micromechanical Mori–Tanaka approach is applied for the prediction of viscosity, and it is concluded that the elasticity-based model fits well with the experimental data. In addition, a semi-empirical model for non-Newtonian viscosity of CNT-dispersed polymer suspensions is proposed. The predictions are verified with experimental results.

Keywords

Viscosity, nanofiber-dispersed polymer, micromechanics

1. Introduction

Extensive attention has been paid to research activities on use of nano-fillers (e.g., carbon nanotubes, carbon nanofibers) as superior candidates for high-performance and multi-functional reinforcements of engineering polymers [1–3]. Enhancement of matrix-dominated mechanical properties of fiber-reinforced plastic (FRP) using nanoparticle-dispersed polymer (e.g., compressive strength, interlaminar fracture toughness, residual strength) has been widely recognized [4–8]. When using nanoparticle-dispersed polymer for FRPs, prepreg-based fabrication, resin transfer molding (RTM), and resin film infusion (RFI) are widely used. Therefore, viscosity of nanoparticle-dispersed polymer suspensions is the key factor that controls the quality and performance of the fabricated composites.

Theoretical studies on viscosity of particle-dispersed suspensions have been conducted for the cases of dilute suspensions of spherical or ellipsoidal particles [9, 10]. It is still a challenge to formulate the theoretical expressions of viscos-

* To whom correspondence should be addressed. E-mail: yokozeki@aastr.t.u-tokyo.ac.jp
Edited by JSCM.

 DOI:10.1163/156855111X610217

ity of non-dilute particle-dispersed suspensions. When we have to consider the orientation of fiber-like particles in suspensions or nonlinear viscous characteristics, the theoretical prediction is also tough work. Thus, numerical simulations (e.g., particle method) and semi-empirical predictions have been widely used for the cases described above [11–13]. Nanofibers are advantageous for the reinforcements of polymer, because the fillers have high aspect ratio (i.e., length divided by diameter). However, simple methods for the prediction of polymer suspensions containing non-dilute nanofibers with orientations have not been established yet. It is important to develop a simple predictive model of viscosity of nanofiber-dispersed polymer suspensions in order to know the quality of composites prior to fabrication. On the other hand, a simpler predictive model gives a way to identify the shapes, orientations and concentrations of nanofibers by measuring the viscous properties of polymer suspensions. Modeling of viscosity of nanofiber-dispersed polymer suspensions is a key issue for the manufacturing of nanocomposites.

The main goal of this research is to apply the micromechanical elasticity model to the prediction of viscosity of nanofiber-dispersed polymer suspensions. Analogy between the shear viscosity and the shear stiffness and correspondence of viscoelasticity to elasticity are well recognized. In this study, it is proposed that the micromechanical Mori–Tanaka model [14] is used for the prediction of viscosity. This approach can handle the non-dilute suspensions and the effect of orientation of nanofibers.

In this paper, the Mori–Tanaka approach is briefly summarized first, and viscosity predictions are compared to the previous experimental data [15] by the present author. In addition, a semi-empirical model is proposed in order to predict the nonlinear viscous properties of nanofiber-dispersed suspensions which were observed in the previous experiment. The proposed semi-empirical model is also verified based on the comparison with the experimental data.

2. Mori–Tanaka Model

Consider non-dilute inclusions in an infinite homogeneous isotropic matrix medium. In the Mori–Tanaka approach [14, 16], the relationship between the average strain of matrix ($\bar{\boldsymbol{\varepsilon}}_0$) and the strain of rth phase of inclusions ($\bar{\boldsymbol{\varepsilon}}_r$) can be expressed using the strain concentration tensor.

$$\bar{\boldsymbol{\varepsilon}}_r = \mathbf{A}_r^{\mathrm{dil}} \bar{\boldsymbol{\varepsilon}}_0, \tag{1}$$

$$\mathbf{A}_r^{\mathrm{dil}} = \left[\mathbf{I} + \mathbf{S}_0 \mathbf{L}_0^{-1} (\mathbf{L}_r - \mathbf{L}_0)\right]^{-1}, \tag{2}$$

where $\mathbf{S}$ denotes the Eshelby tensor, $\mathbf{L}$ is a stiffness tensor, and $\mathbf{I}$ is the identity tensor. Subscript 0 denotes the matrix. Straight nanofibers with aspect ratio, α, can be regarded as slender prolate spheroids. The Eshelby tensor of prolate spheroidal inclusions is given in the Appendix, when the fiber axis coincides with the axis-3. Based on the average strain theorem, the relationship between the average strain

of composite ($\bar{\boldsymbol{\varepsilon}}$) and the strain of rth phase of inclusions ($\bar{\boldsymbol{\varepsilon}}_r$) can be expressed as

$$\bar{\boldsymbol{\varepsilon}}_r = \mathbf{A}_r \bar{\boldsymbol{\varepsilon}}, \tag{3}$$

$$\mathbf{A}_r = \mathbf{A}_r^{\mathrm{dil}} \left(\sum_r v_r \mathbf{A}_r^{\mathrm{dil}} \right)^{-1}. \tag{4}$$

Herein, the volume fraction of the rth phase of inclusion is denoted as v_r. Equations (3) and (4) are valid when r is set to be 0 (i.e., in the case of the matrix phase). The overall stiffness tensor of composites can be written as

$$\mathbf{L}_c = \sum_r v_r \mathbf{L}_r \mathbf{A}_r = \sum_r v_r \mathbf{L}_r \mathbf{A}_r^{\mathrm{dil}} \left(\sum_r v_r \mathbf{A}_r^{\mathrm{dil}} \right)^{-1}. \tag{5}$$

When the orientation distribution of nanofibers is considered, the overall stiffness can be expressed as

$$\mathbf{L}_c = \sum_r v_r \left\{ \mathbf{L}_r \mathbf{A}_r^{\mathrm{dil}} \right\} \left(\sum_r v_r \left\{ \mathbf{A}_r^{\mathrm{dil}} \right\} \right)^{-1}, \tag{6}$$

$$\{\mathbf{L}\} = \int_\phi \int_\theta \int_\varphi L_{mnpq} m_{mi} m_{nj} m_{pk} m_{ql} n(\phi, \theta, \varphi) \sin\theta \, \mathrm{d}\phi \, \mathrm{d}\theta \, \mathrm{d}\varphi, \tag{7}$$

where $\{\cdot\}$ denotes averaging over all possible directions, m_{ij} is coordinate transformation tensor, and $n(\varphi, \theta, \psi)$ is the orientation distribution function defined in Eulerian coordinates. In the case of three-dimensionally random distribution, $n(\varphi, \theta, \psi)$ is equal to $1/(8\pi^2)$.

3. Prediction of Viscosity and Comparison with Experimental Results

3.1. Nanofibers in Polymer Suspensions

The lengths of nanofibers generally have a distribution, and thus, aspect ratios of nanofibers are not constant in polymer suspensions. It was shown that carbon nanofibers in polymer suspensions used in the previous experimental study [15, 17] have various lengths. In this study, it is assumed that nanofibers have constant aspect ratio. In addition, every nanofiber is assumed to be straight and isolated in polymer suspensions, although nanofibers generally agglutinate and have curvatures. Three-dimensionally random distribution is assumed for the orientation of nanofibers in polymer.

3.2. Comparison with Experimental Results of Viscosity

In this study, the evaluated shear stiffness using equation (6) is regarded as the viscosity of nanofiber-dispersed polymer suspensions based on the analogy between the shear viscosity and the shear stiffness. The densities of resin and carbon

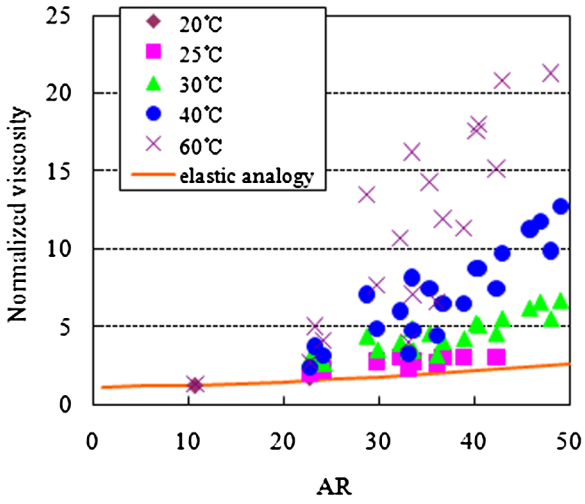

Figure 1. Normalized viscosity at shear rate of 100 s^{-1} as a function of aspect ratio of carbon nanofiber. This figure is published in color in the online version.

nanofiber are set to be 1.16 and 2.1 g/cm^3, respectively. It is assumed that carbon nanofibers are stiff enough compared to resin, and matrix resin (uncured resin) is incompressible (i.e., Poisson's ratio of matrix resin is set to be nearly equal to 0.5).

In the previous experimental study [15], viscous properties of 5 wt% cup-stacked carbon nanofiber-dispersed epoxy suspensions were measured by a cone–plate viscometer. It was shown that pure epoxy resin is a Newtonian fluid, but carbon nanofiber-dispersed epoxy suspensions exhibit non-Newtonian fluid behavior. The predicted viscosity is compared to the experimental shear viscosity at shear rate of 100 s^{-1}, as shown in Fig. 1. The vertical axis shows the viscosity of nanofiber-dispersed suspensions divided by that of pure epoxy (this value is called the normalized viscosity in this study), and the horizontal axis shows the aspect ratio of carbon nanofibers. Measured data at 20, 25, 30, 40 and 60°C are used for comparison. The experimental data at higher temperature exhibit considerable variation and higher normalized viscosity. This phenomenon results from the following arguments: aggregation of carbon nanofibers disappear at high shear rates, and every carbon nanofiber is isolated [15]; when the shear rate increases enough, the dispersion state of carbon nanofibers is stabilized; the dependence of viscosity on the shear rate disappears at high shear rates, and the viscosity decreases and converges to the steady-state viscosity as shown in Fig. 2. This dependence is also observed in the case of particle-dispersed suspensions [18]; when temperature increases, a higher shear rate is needed for complete isolation of nanofibers because aggregation of nanofibers is susceptible to formation at high temperature; however, the maximum shear rate in the previous study is 100 s^{-1}; as a result, carbon nanofibers are not isolated at the shear rate of 100 s^{-1} in the case of high temperature, and it is con-

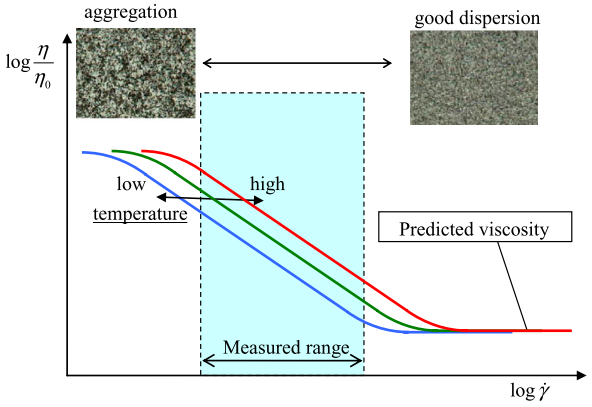

Figure 2. Schematic of viscosity–shear rate curve in relation to dispersion state and temperature. This figure is published in color in the online version.

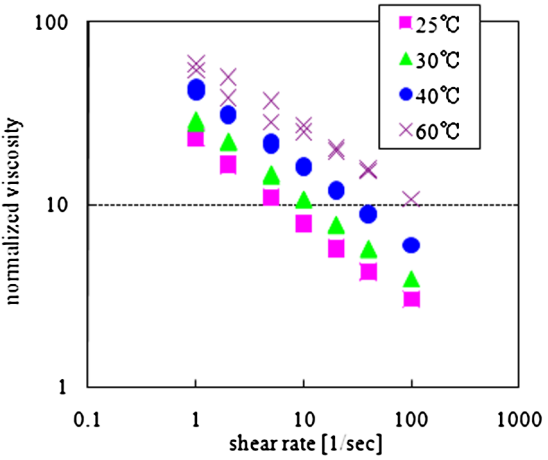

Figure 3. Viscosity–shear rate curve of nanofiber-dispersed epoxy ($AR = 32$). This figure is published in color in the online version.

sidered that the experimental data at higher temperature exhibit higher normalized viscosity. In Fig. 3, viscosity–shear rate curves of carbon nanofiber-dispersed epoxy (aspect ratio of 32) at various temperatures [15] are presented. The experimental data coincide with the tendency shown in Fig. 2. In this study, it is considered that the experimental data at the shear rate of 100 s^{-1} at lower temperatures correspond to the steady-state viscosity. As the predicted model assumes complete dispersion of carbon nanofiber in polymer suspensions, experimental data at lower temperatures are considered to be suitable for comparison to the predictions in this study.

Looking at Fig. 1 again, we can conclude that the predictions based on elastic analogy (solid line) agree well with the experimental data at 20, 25 and 30°C. If complete dispersion of carbon nanofibers is achieved, experimental data at high temperatures may show lower normalized viscosities and approach the predicted

values. It is concluded that the steady-state viscosity at high shear rates can be predicted using the elastic micromechanical model.

4. Semi-empirical Model of Non-Newtonian Suspensions

4.1. Exponential Relation

In the previous study [15], non-Newtonian behavior was observed in the cases of nanofiber-dispersed epoxy suspensions, and the following exponential form of viscosity (η)–shear rate ($\dot{\gamma}$) curve was applied to the experimental results.

$$\eta = C\dot{\gamma}^{-n}. \tag{8}$$

It was shown that a master curve was obtained to express the relationship between the exponent, n, and aspect ratio, AR, of carbon nanofibers, when the concentration of nanofiber was fixed. Specifically, in the case of 5 wt% carbon nanofiber-dispersed suspensions, the following empirical equation was obtained based on the significant number of experimental results.

$$n = 0.6(1 - \mathrm{e}^{-0.0002(AR-1)^{2.5}}). \tag{9}$$

This equation may vary depending on the concentration and the surface treatment of carbon nanofibers. In the following section, a simple method to predict the non-Newtonian behavior of nanofiber-dispersed suspensions is explained when the relation like equation (9) is obtained experimentally.

4.2. Semi-empirical Model

As shown in Section 3.2, the elasticity-based analogy model can be used for prediction of the steady-state viscosity of nanofiber-dispersed suspensions at high shear rates. Non-Newtonian behavior at intermediate shear rates was expressed by the exponential form as shown in Section 4.1, and the master curve (i.e., equation (9)) was obtained experimentally. Therefore, the following bi-linear form of non-Newtonian viscosity is assumed here as shown in Fig. 4.

$$\begin{cases} \eta = \eta_{\mathrm{pred}}\left(\dfrac{\dot{\gamma}}{\tilde{\dot{\gamma}}}\right)^{-n} & (\dot{\gamma} \leqslant \tilde{\dot{\gamma}}), \\ \eta = \eta_{\mathrm{pred}} & (\dot{\gamma} \geqslant \tilde{\dot{\gamma}}). \end{cases} \tag{10}$$

In this equation, η_{pred} is predicted by Mori–Tanaka model, and the exponent, n, is given empirically (i.e., equation (9)). It should be noted that $\tilde{\dot{\gamma}}$, which defines the intersection of the bi-linear model, is a function of temperature and other parameters. In this study, $\tilde{\dot{\gamma}}$ is assumed to be a function of temperature, and is determined by comparison to experimental results.

A viscosity–shear rate curve of 5 wt% carbon nanofiber ($AR = 39$) dispersed suspensions is shown in Fig. 5, and compared to the experimental results. In this prediction, $\tilde{\dot{\gamma}}$ is set to be 200 s^{-1} at 25°C, 300 s^{-1} at 30°C, 1000 s^{-1} at 40°C

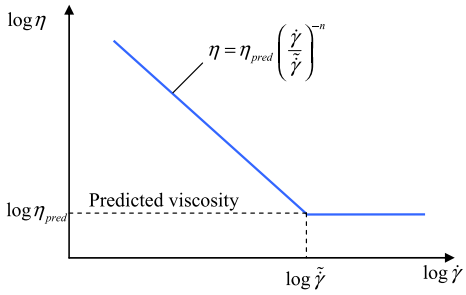

Figure 4. Bi-linear model for non-Newtonian viscosity. This figure is published in color in the online version.

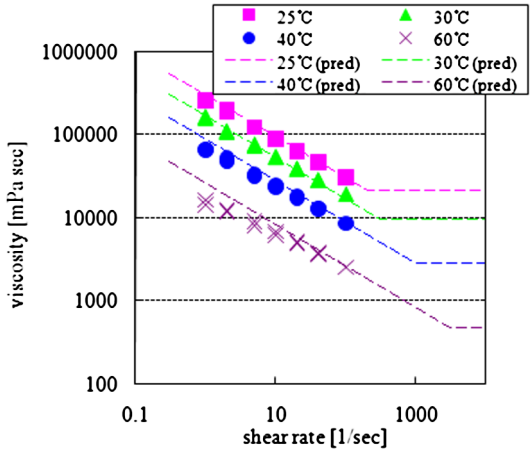

Figure 5. Comparison of viscosity–shear rate curves between fitted predictions and experiments ($AR = 39$). This figure is published in color in the online version.

and 3000 s^{-1} at 60°C. Using these parameters, comparison between the prediction and the experiment is made for the cases of $AR = 24$ and $AR = 34$, as shown in Fig. 6. It is concluded that predictions of viscosity based on the proposed semi-empirical model agree well with the experimental non-Newtonian behavior of carbon nanofiber-dispersed suspensions.

The proposed semi-empirical model utilizes the micromechanical theoretical model for the prediction of steady-state viscosity at high shear rate, η_{pred}, whereas the exponent, n, and the intersection of the bi-linear model, $\tilde{\dot{\gamma}}$, are determined based on the experimental data. This semi-empirical model assumes that parameters depend on only aspect ratio and concentration of carbon nanofibers, and are independent of type of material system. Many issues are further to be investigated. For example, it is necessary to investigate effects of interfacial treatment of nanofibers, variation of aspect ratio of nanofibers (this study assumes constant aspect ratio in the prediction), orientation of nanofibers in suspensions, and aggregation of nanofibers on the viscosity of suspensions. Numerical simulation and

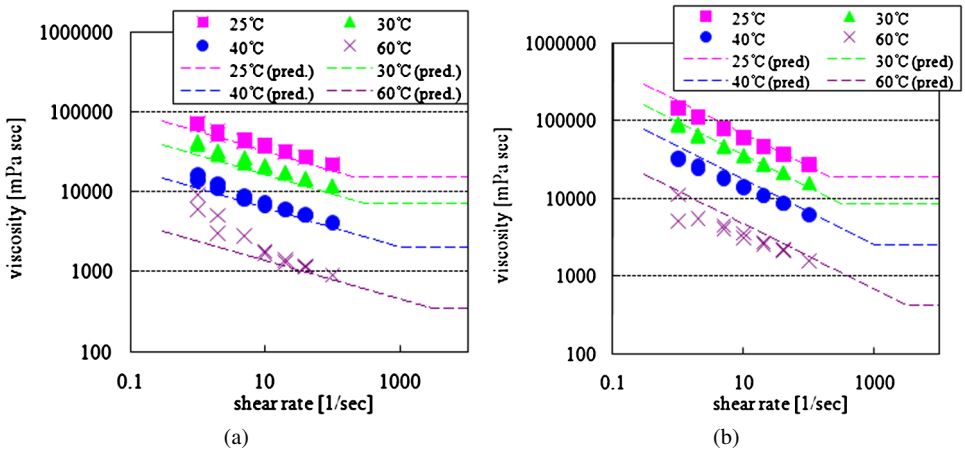

Figure 6. Comparison of viscosity–shear rate curves between predictions and experiments: (a) $AR = 24$, (b) $AR = 34$. This figure is published in color in the online version.

additional experimental studies are also important in order to verify the proposed model in more details.

5. Conclusions

In this study, the micromechanical Mori–Tanaka model was applied to the prediction of viscosity of nanofiber-dispersed suspensions. Comparison between the prediction and the previous experimental data indicated that prediction based on shear stiffness can be applied to the estimation of steady-state viscosity of nanofiber-dispersed suspensions at higher shear rate.

A semi-empirical bi-linear model for non-Newtonian viscosity of nanofiber-dispersed suspensions was also proposed. The shear stiffness-based prediction was applied to steady-state viscosity at higher shear rate, and the empirical exponential model was used in the proposed model. It was shown that the predicted non-Newtonian viscosities agree well with the experimental data. The proposed model is able to predict the viscosity of nanofiber-dispersed suspensions including non-Newtonian behavior, and contributes to the fundamental knowledge of application of nanofiber-dispersed polymer to composites and manufacturing process of nanofiber-based materials.

Acknowledgements

The author wishes to thank Mr. Chawin Jitpipatpong from the University of Tokyo, Dr. Takashi Yanagisawa, Mr. Masaru Ishibashi, Ms. Akiko Arai, Mr. Koichi Kimura and Mr. Kazuo Kimura from GSI Creos Corporation, and Mr. Akito Kawasaki from Arisawa Manufacturing Co. Ltd, for providing and discussing the experimental data referred in this paper.

References

1. E. T. Thostenson, Z. Reng and T.-W. Chou, Advances in the science and technology of carbon nanotubes and their composites: a review, *Compos. Sci. Technol.* **61**, 1899–1912 (2001).
2. D. M. Delozier, K. A. Watson, J. G. Smith and J. W. Connell, Preparation and characterization of space durable polymer nanocomposite films, *Compos. Sci. Technol.* **65**, 749–755 (2005).
3. T. Ogasawara, Y. Ishida, T. Ishikawa, T. Aoki and T. Ogura, Helium gas permeability of montmorillonite/epoxy nanocomposites, *Composites Part A* **37**, 2236–2240 (2006).
4. Y. Iwahori, S. Ishiwata, T. Sumizawa and T. Ishikawa, Mechanical properties improvements in two-phase and three-phase composites using carbon nano-fiber dispersed resin, *Composites Part A* **36**, 1430–1439 (2005).
5. A. K. Subramaniyan and C. T. Sun, Enhancing compressive strength of unidirectional polymeric composites using nanoclay, *Composites Part A* **37**, 2257–2268 (2006).
6. M. H. G. Wichmann, J. Sumfleth, F. H. Gojny, M. Quaresimin, B. Fiedler and K. Schulte, Glass-fibre-reinforced composites with enhanced mechanical and electrical properties — benefits and limitations of a nanoparticle modified matrix, *Eng. Fract. Mech.* **73**, 2346–2359 (2006).
7. T. Yokozeki, Y. Iwahori and S. Ishiwata, Matrix cracking behaviors in carbon fiber/epoxy laminates filled with cup-stacked carbon nanotubes (CSCNTs), *Composites Part A* **38**, 917–924 (2007).
8. N. A. Siddiqui, R. S. C. Woo, J.-K. Kim, C. R. Y. Leung and A. Munir, Mode I interlaminar fracture behavior and mechanical properties of CFRPs with nanoclay-filled epoxy matrix, *Composites Part A* **38**, 449–460 (2007).
9. A. Einstein, Eine neue bestimmung der moleküldimensionen, *Annalen der Physik* **19**, 289–306 (1906).
10. G. B. Jeffery, The motion of ellipsoidal particles immersed in a viscous fluid, *Proc. Roy. Soc. London* **A102**, 161–179 (1922).
11. J. F. Douglas and E. J. Garboczi, Intrinsic viscosity and the polarizability of particles having a wide range of shapes, *Adv. Chem. Phys.* **XCI**, 85–153 (1995).
12. J. Bicerano, J. F. Douglas and D. A. Brune, Model for the viscosity of particle dispersions, *Polym. Rev.* **39**, 561–642 (1999).
13. S. Yamamoto, Development and application of the particle simulation method for fiber and plate-like particle dispersed systems, *J. Soc. Rheology Japan* **29**, 185–190 (2001) (in Japanese).
14. T. Mori and K. Tanaka, Average stress in matrix and average elastic energy of materials with misfitting inclusions, *Acta Metall.* **21**, 571–574 (1973).
15. T. Yokozeki, C. Jitpipatpong, A. Arai, M. Ishibashi, T. Yanagisawa, A. Kawasaki, T. Takahashi and T. Aoki, Evaluation of viscosity of CNT-dispersed polymer under various processing conditions, *J. Japan Soc. Compos. Mater.* **36**, 19–25 (2010) (in Japanese).
16. J. Wang and R. Pyrz, Prediction of the overall moduli of layered silicate-reinforced nanocomposites — part I: Basic theory and formulas, *Compos. Sci. Technol.* **64**, 925–934 (2004).
17. T. Yokozeki, C. Jitpipatpong, T. Aoki, A. Arai, M. Ishibashi and T. Yanagisawa, Effect of milling process on CNT length and rheological/mechanical properties of nanocomposites, *J. Nanostruct. Polym. Nanocompos.* **6**, 5–11 (2010).
18. K. Osaki, *Rheology*. Kogyo Chosakai, Tokyo (2004) (in Japanese).

Appendix

A1. Eshelby Tensor

Consider a prolate spheroidal inclusion in an isotropic matrix. The long axis direc-

tion coincides with the axis-3 herein. The aspect ratio of the inclusion (or nanofiber) and Poisson's ratio of matrix are denoted as α and ν, respectively. Each component of Eshelby tensor is given by

$$\begin{gathered}
S_{1111} = S_{2222} = QI_{12} + RI_1, \\
S_{1122} = S_{2211} = QI_{12} - RI_1, \\
S_{1133} = S_{2233} = \alpha^2 QI_{13} - RI_1, \\
S_{3311} = S_{3322} = QI_{13} - RI_1, \\
S_{3333} = \alpha^2 QI_{33} + RI_3, \\
S_{2323} = S_{3131} = \frac{1+\alpha^2}{2} QI_{13} + \frac{1}{2} R(I_1 + I_3), \\
S_{1212} = QI_{12} + RI_1, \\
\text{else } S_{ijkl} = 0, \\
Q = \frac{3}{8\pi(1-\nu)}, \qquad R = \frac{1-2\nu}{8\pi(1-\nu)},
\end{gathered} \tag{A.1}$$

where the parameters in (A.1) are expressed as

$$\begin{gathered}
I_1 = 2\pi\alpha \frac{\alpha\sqrt{1-\alpha^2} - \cosh^{-1}\alpha}{(1-\alpha^2)^{3/2}}, \\
I_3 = 4\pi - 2I_1, \\
I_{33} = \frac{4\pi}{3} \frac{1}{\alpha^2(\alpha^2-1)} \left(\frac{4\pi}{3} - I_3 \right), \\
I_{13} = \frac{1}{2(\alpha^2 - a)} \left(\frac{4\pi}{3} - I_1 \right), \\
I_{12} = \frac{1}{4} \left(\frac{4\pi}{3} - I_{13} \right), \\
I_{33} = 3I_{12}.
\end{gathered} \tag{A.2}$$